Neural-Network-Based Signature Recognition for Harmonic Source Identification

D. Srinivasan, *Senior Member, IEEE*, W. S. Ng, and A. C. Liew, *Senior Member, IEEE*

***Abstract*—This paper proposes a neural-network (NN)-based approach to nonintrusive harmonic source identification. In this approach, NNs are trained to extract important features from the input current waveform to uniquely identify various types of devices using their distinct harmonic "signatures." Such automated, noninvasive device identification will be critical in future power-quality monitoring and enhancement systems. Several NN-based classification models including multilayer perceptron (MLP), radial basis function (RBF) network, and support vector machines (SVM) with linear, polynomial, and RBF kernels were developed for signature extraction and device identification. These models were trained and tested using spike train data gathered from the Fourier analysis of the input current waveform in the presence of multiple devices. The performance of these models was compared in terms of their accuracy, generalization ability, and noise tolerance limits. The results showed that MLPs and SVM were both able to determine the presence of devices based on their harmonic signatures with high accuracy. MLP was found to be the best signature identification method because of its low computational requirements and ability to extract the information necessary for highly accurate device identification.**

***Index Terms*—Artificial neural network (ANN), power harmonics, signature identification.**

I. Introduction

THE WIDE USE of nonlinear loads, such as personal computers, monitors, laser printers, variable speed drives, UPS systems, and other electronic equipment has made harmonics a major issue in commercial and industrial power distribution systems—especially when these are found in high densities. Any distribution system servicing high-density nonlinear loads is vulnerable to problems of power quality such as equipment malfunction, poor power factor, voltage wave distortion, and component failure.

There has been a rapid increase in the number and power rating of such highly nonlinear power-electronic devices used in power distribution systems [1]–[4]. Nonlinear loads draw current in a nonsinusoidal manner because their impedance varies when the applied voltage changes during an ac power cycle. The IEEE Standard 519-1992 (IEEE Recommended Practices and Requirements for Harmonic Control in Electrical Power Systems) has established a set of limits to the acceptable level of current harmonics in the power system which ensures that each power consumer plays his or her part in keeping the harmonic distortion levels low.

A commonly used approach to harmonic source detection is to remove shunt capacitors in order to eliminate possible redirection of harmonic flow before performing analysis [1]–[3]. However, this approach may give rise to undervoltage problems and missing resonance phenomena in some cases [5]. In [6] and [7], state estimation technique with least-square estimators to identify the location of harmonic sources using observability analysis were used. Reference [8] employed a Kalman filter estimation model with the harmonic injection as a random state variable for harmonic source identification. Error covariance analysis of harmonic injection was used to determine the optimal metering locations.

Nonintrusive monitoring of residential loads using the input current waveform was used in [9] and [10], where appliance signatures were used for monitoring residential loads. In these studies, current waveform amplitudes and load cycles were used for device identification. The step changes in the steady-state aggregate complex power consumption of various commonly used electrical devices were plotted in the *P-Q* chart. Different regions of the *P-Q* plane represented different devices and formed the feature vector of the devices. The positive and negative clusters of the *P-Q* chart were matched to correspond to the on and off state changes of the electrical devices, respectively. In [10], other information such as the modeling of the state transition cycles of a device, functional sequences of a group of devices, and the time of event that may determine the likelihood of a device being used were associated to the *P-Q* chart for better identification accuracy. Reference [11] proposed a feature vector consisting of the time-domain waveform of detected transients to be compared with waveform templates that were shifted in time, or offset in magnitude. However, accurate device identification was not always possible as transients remain difficult to detect and analyze. Additionally, the identification techniques presented in [9]–[11] required human intervention to sort the data obtained and to detect important characteristics in the waveform.

This paper investigates the application of neural-network (NN)-based models on nonintrusive signature identification, without human intervention. Because of the differing ways in which a device conditions the electrical power supply, different categories of devices may produce different types of current harmonics. In this paper, this information is treated as a unique signature of the device, distinct from that of other devices. The waveform distortion caused by nonlinear loads is quantified in the frequency domain by applying Fourier analysis, and used to nonintrusively detect the presence of various devices in the

Manuscript received August 20, 2003; revised August 31, 2004. This work was supported by the National University of Singapore under Research Grant R-263-000-190-112. Paper no. TPWRD-00414-2004.

The authors are with the Department of Electrical and Computer Engineering, National University of Singapore, Singapore 119260 (e-mail: dipti@nus.edu.sg; g0203557@nus.edu.sg; elelac@nus.edu.sg).

Digital Object Identifier 10.1109/TPWRD.2005.852370

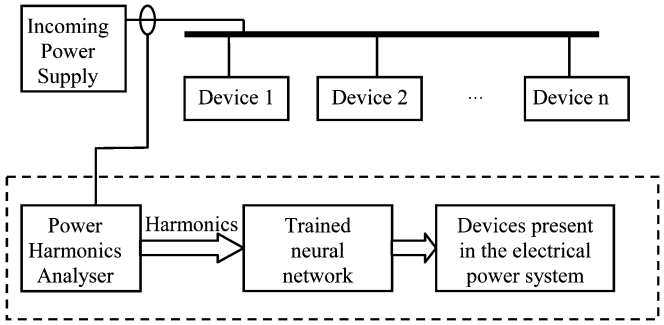

Fig. 1. Device identification system.

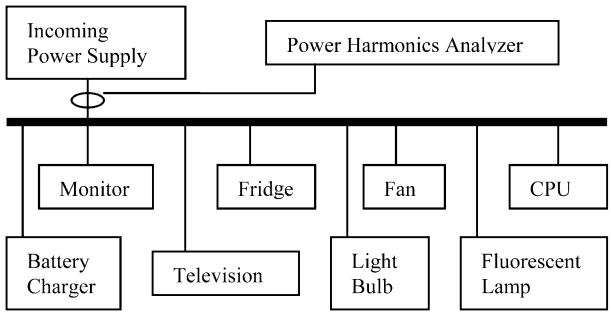

Fig. 2. Experimental setup.

electrical installation. The unique device signature can be used to provide accurate information to power-quality management and enhancement systems so that appropriate remedial action can be taken. It is envisaged that such automated, noninvasive device identification will be critical in future power-quality monitoring and enhancement systems.

The classification and function approximation capabilities of artificial neural networks (ANNs) have been employed in power-quality studies, fault, and harmonics source classification [13]–[17]. In other studies, the support vector machine (SVM) model has shown potential in power harmonics related pattern recognition [18], [19]. Among the benefits derived from the parallel structure of ANN is their ability to recognize nonlinear functions, the ability to adapt to different environments, and their high noise tolerance [12].

This paper evaluates harmonic components as sources of valuable information for signature identification. Several NNs-based signature identification models including the multilayer perceptron (MLP), radial basis function (RBF) network, and support vector machines (SVM) with linear, polynomial, and RBF kernels were developed. These models were trained using spike train data gathered from Fourier analysis of the input current waveform in the presence of multiple devices and instructed to produce corresponding output to indicate the devices present in electrical installation. Once trained, these models could identify the devices present when presented with the current harmonics of the power source. A comparison of performance showed that multilayer perceptron and SVM-based models were both able to determine the presence of devices based on their harmonic signatures with high accuracy. MLP was, however, found to be the best signature identification method because of its ability to accurately extract the necessary information for device identification and because of its low computational requirements.

II. Device Signature Identification System

This paper investigates the application of NN-based models on nonintrusive signature identification, without human intervention. The harmonic components of current are used as sources of valuable information for signature identification. Finally, the trained ANN or SVM was used to identify the devices present from just the current harmonics at the power source. The overall scheme is shown in Fig. 1.

The process is carried out in the following steps. The implementation of these processes is explained in detail in the following sections.

A. Data Capture and Preprocessing

In order to form the signature to represent an electrical device, information obtained from the current measurements of the incoming electrical supply was used to form a feature vector which was converted into a standard format using the power harmonics analyzer.

B. Feature Extraction

The process of extracting key information from the harmonic representations of the signature was performed using NN-based models. The extracted features are matched with the templates stored in NN memory.

C. Performance Evaluation

Based on the similarity of the new data with the templates, a decision is made by thresholding the fit value to indicate the presence of a device.

It is essential that the signature identification system keeps to a minimum both for the computing complexity and the amount of data required for verification.

III. Data Capture and Preprocessing

An experimental laboratory setup was created to represent an electrical installation with commonly used devices. For the initial phase of the experiment, eight single-phase devices were connected in parallel using the laboratory's existing electrical wiring (Fig. 2). Measurements were made at the main incoming source of the laboratory using the Fluke 41 power harmonics analyzer.

With eight devices, the authors were able to obtain 256 discrete states, each representing different combinations of devices switched on. These eight devices were switched on and off in steps to allow current waveform measurement of all possible combinations. For each combination, a total of 18 readings (each 10 s apart) were recorded. The Fluke 41 power harmonics analyzer immediately calculates the harmonics content (amplitude and phase) of the current waveform through fast Fourier transform (FFT).

In the experiments, only the odd-numbered harmonics, from the fundamental to the 15th harmonic, of the current waveforms were of significant amplitude. Therefore, only the first eight odd

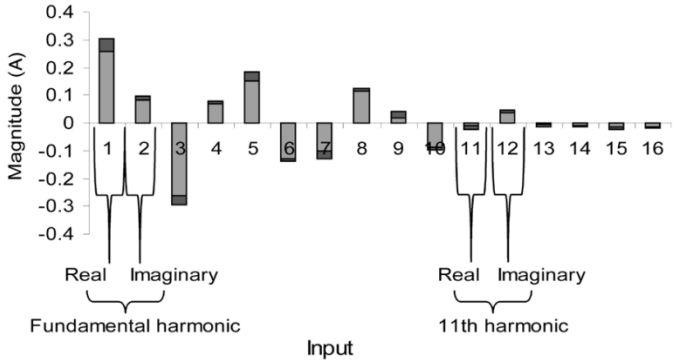

Fig. 3. Signature identification feature vector.

harmonics (fundamental, third, fifth, seventh, ninth, 11th, 13th, 15th) were recorded. For ease of representation, the amplitude and phase angles of the harmonics were converted into complex representation, where each harmonic had a real and an imaginary part.

With eight harmonics taken into consideration, the feature vector presented to the ANN will have 16 inputs given by the following equations:

$$x_i = I_{(i+1)/2}\cos\phi_{(i+1)/2}, \quad \text{for } i = 1,3,5,7,9,11,13, \text{ and } 15 \tag{1}$$

$$x_i = I_{i/2}\sin\phi_{i/2}, \quad \text{for } i = 2,4,6,8,10,12,14, \text{ and } 16 \tag{2}$$

where x_i is the ith input, I_n is the magnitude of the nth odd current harmonic, and ϕ_n is the phase angle of the nth odd current harmonic.

Fig. 3 illustrates how x_1 and x_2 of the input vector were calculated from the real and imaginary parts of the fundamental harmonic according to (1) and (2), respectively. For example, the real and imaginary parts of the 11th harmonic are labeled as x_{11} and x_{12}, respectively.

IV. Harmonics Signature Characteristics

The harmonic amplitude and phase of the devices were found to fluctuate in a small and random manner with respect to time. This could be due to fluctuations in the source power supply or to electrical characteristics inherent in the devices. The source voltage measured over the period of experiments had a mean of 231.5 V, a standard deviation of 1.26 V, and higher harmonic contents of below 1.5% of the fundamental.

The effect of the eight loads on the source voltage was negligible since the wiring resistances were small.

Apart from these random fluctuations, most of the devices had either short transient states or were capable of multiple modes of operation that may have produced significantly different signatures. As a result, for the purpose of this experiment, all of the devices were set to operate in a specific mode and only steady-state current harmonics were taken into consideration. This limitation is fair because in actual operation, these devices are expected to operate in a specific mode for large proportions of their operating time.

Fig. 4 shows the distinctive harmonic signatures of all the devices in the experimental setup. The fluctuation ranges of the harmonics components are also shown. The monitor, central processing unit (CPU), and television use the switch-mode power supply, which produces high third and fifth current harmonics with amplitudes at times exceeding those of the fundamental frequency waveform.

The computer's CPU showed the largest fluctuation in the ratio of magnitude to mean harmonic amplitude. This is because of the large number of different electrical components inside the CPU that draw independent amounts of current from the CPU's power supply. The CPU was set to a constant operation for consistency (the repeated playing of an audio file) while measuring various combinations of devices. On the other hand, resistive loads such as the light bulb show low harmonic distortion but have characteristically higher power consumption compared to the other devices. The monitor and CPU show largely similar-shaped signature patterns but are different in terms of magnitude.

Fig. 5 shows the average ratio of the fluctuations to the mean harmonic amplitude, calculated from all possible combinations of devices. The spikes at input 9 and 16 were caused by the characteristics of a few devices including the monitor and CPU that demonstrated exceptionally large fluctuations in the ninth and 13th harmonics. If the fluctuations are treated as noise and the mean harmonic amplitude is treated as the original signal, the signal-to-noise ratio (SNR) is found to be above 2 for most inputs. The SNR is low for the 13th and 15th harmonics (input 13 to 16) because of the smaller signal amplitude.

The NN models are expected to be able to perform well under these SNR conditions, and were thus chosen to perform the signature identification in the next step.

V. NN-Based Models

A. Multilayer Perceptron

The single-hidden-layer MLP model [12] was used for identification and classification of the devices present. The nodes of the hidden layer were fully connected to those in the input layer and the output layer. The number of input nodes in the MLP NN depends on the number of harmonics taken into consideration. Each harmonic requires two nodes for the real and imaginary parts of its complex representation. Starting with the fundamental frequency represented by the first two input nodes, the number of inputs nodes was sequentially increased by adding higher order harmonics. The optimum number of input neurons was determined by measuring the effectiveness of the additional harmonics taken into consideration. The number of hidden nodes was also varied from 4 to 60 to determine the optimum configuration for the NN. The best number of inputs and hidden nodes were 16 and 20, respectively.

The number of output nodes depends on the number of classes to be identified which, in this case, is the number of devices to be classified in the experiment. Hence, with an initial setup of eight devices, the number of output nodes was fixed at 8. The final outputs of the neural networks were passed through a *signum* function that converted all positive values to the integer $+1$ (device is present) and all negative values to -1 (device is absent).

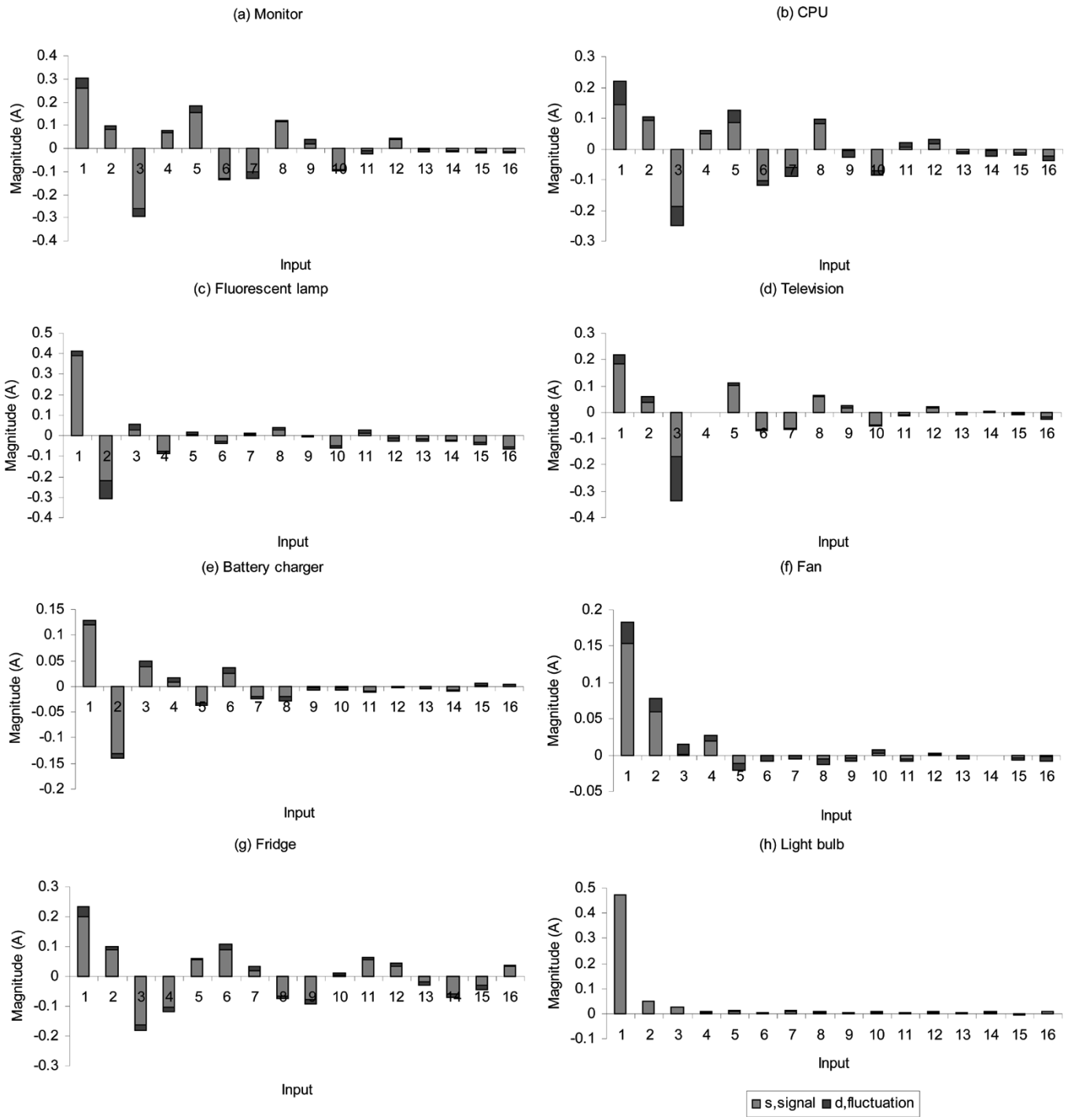

Fig. 4. Harmonic signatures of various devices.

Several training algorithms, including the gradient descent with momentum and resilient backpropagation training algorithms [12], were tested in the training of the MLP. Resilient backpropagation was found to perform significantly better than the gradient descent method.

B. RBF NN

Like the MLP, the RBF NN is a universal classifier and nonlinear function approximator. While being structurally similar, the fundamental difference between the RBF NN and MLP lies in the way the hidden neurons combine inputs from the preceding layers in the network; the MLP uses the inner products whereas RBF uses the Euclidean distance [12].

In this paper, the structure of the RBF NN was similar to the MLP described above. The number of input neurons in the RBF NN was selected to be 16. The optimum number of hidden nodes for the RBF neural networks was experimentally determined by sequentially adding the nodes based on maximum variance. The RBF hidden neurons used the Gaussian function with width parameter σ equal to 1. The number of output nodes was fixed to be 8 for the first experiment.

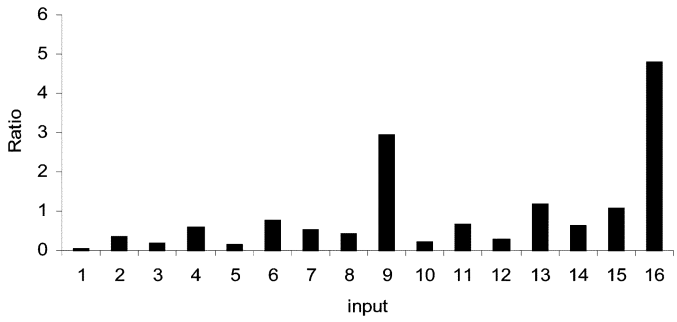

Fig. 5. Ratio of fluctuation to the mean harmonic amplitude.

C. SVM-Based Model

Several SVM models were implemented in various configurations to obtain the best configuration for each experimental setup. Performance with various kernels including the linear, polynomial, and RBF kernels [12] was compared. When using the linear kernel, SVM performs the classification in the original input vector space. The polynomial and RBF kernels perform the classification in the higher order polynomial space and Gaussian function space, respectively.

In the experiments, the input vector to the SVM-based classifier was fixed at 16 (with eight harmonics taken into consideration). The cost parameter was slowly varied from 0.3 to 1.5. Polynomial kernels of degrees ranging from 2 to 5 were compared while the widths of the RBF functions (gamma) were varied from 0.5 to 3.0.

Outputs from the SVM-based model were passed through the signum function to be converted to $+1$ or -1, just as they were for the MLP-based model.

Since SVM is inherently a two-class classifier, for this multiclass problem in device signature identification, several approaches were tested to extend the SVM into a multiclass classifier. The "one against many" technique [12] was finally adopted in this work. The best SVM models were then used for identifying the presence or absence of each device.

VI. Training and Performance Evaluation

Several stages of training and testing were carried out on the data readings collected from the initial setup of eight devices. In the first stage, the laboratory measurements (to be referred to as the original data set from here onwards) were split randomly into training and testing data to test the ability of the MLP, RBF, and SVM-based models to classify the presence or absence of combinations of several devices, after receiving training on all possible scenarios. In the second stage, the focus was on the models' ability to predict combinations of devices after generalizing from the current harmonics for a single device. Finally, random noise of maximum magnitude was added to the original data set to test the noise tolerance of the models.

A. Training Using Laboratory Measurements

In this stage, the original data set was split such that 66% of the data was used for training and the remainder was used for validation. A K-fold validation test [7] was performed on the entire training data set. For this, the training data were divided into k nonoverlapping subsets. The SVM model was then trained on the whole training data excluding the kth subset. Then, performance of the obtained SVM classifier was estimated on the excluded kth subset. This procedure was repeated for every subset and average performance of the SVM classifier was estimated by tuning the parameters to achieve maximum average classification performance.

TABLE I
Classification Accuracy When Using Laboratory Measurements

Device	MEASUREMENTS				
	Accuracy (%)				
	MLP	RBF	SVM		
			Linear	Polynomial	RBF
Monitor	100	100	99.1	99.5	99.5
CPU	99.9	99.8	95.8	99.6	99.2
Fluo. lamp	99.9	99.8	99.7	99.8	99.8
TV	99.6	99.8	86.0	98.9	97.3
Charger	99.9	99.7	99.6	99.8	99.7
Fan	99.9	99.9	57.0	95.4	82.2
Fridge	99.8	99.7	99.9	100	99.9
Light bulb	100	99.8	99.7	99.7	99.7

TABLE II
Classification Accuracy When Using Mean of Laboratory Measurements

Device	MEASUREMENTS				
	Accuracy (%)				
	MLP	RBF	SVM		
			Linear	Polynomial	RBF
Monitor	99.9	99.9	94.9	99.5	97.7
CPU	99.4	99.8	77.9	98.5	89.3
Fluo. lamp	99.9	99.9	100	100	100
TV	99.0	99.9	67.5	92.0	70.4
Charger	99.8	99.9	97.4	99.8	99.4
Fan	99.8	98.9	58.6	84.1	58.4
Fridge	99.9	100	100	100	100
Light bulb	100	99.9	99.8	100	99.9

Table I shows the test results. For each test sample, the MLP and RBF-based signature identification model correctly classified all of the devices at once. The percentage of correct classifications was calculated by dividing the number of correct classifications (the presence or absence of a device) by the size of the validation set. All classifiers showed excellent classification results.

In further tests, instead of using samples from the original data set for training, the means of each combination were calculated from the original data set. Only 256 means (one for each combination) were used for training, while the whole of the original data set was used for testing the classifiers. Table II shows the test results. All classifiers again showed excellent classification results. The reduction in the size of the training set also reduced the training time required by a considerable factor—especially for the RBF- and SVM-based models that perform quadratic-programming (QP) optimization.

The results prove the ability of NN-based models to generalize well even in the presence of fluctuations in measurement of current harmonics and high SNR.

B. Training Using Mathematically Created Training Set

Theoretically, since all of the electrical devices in the experimental setup were connected in parallel and were electrically

TABLE III
CLASSIFICATION ACCURACY WHEN USING MATHEMATICALLY CREATED TRAINING SET

Device	Accuracy (%)				
	MLP	RBF	SVM		
			Linear	Polynomial	RBF
Monitor	98.9	99.8	92.5	99.4	98.7
CPU	78.7	87.4	74.3	74.5	75.0
Fluo. Lamp	100	99.5	99.9	99.9	99.9
TV	76.4	88.0	63.6	90.5	78.5
Charger	77.5	65.1	69.7	71.7	70.3
Fan	66.5	69.1	66.0	68.0	68.4
Fridge	99.5	98.8	99.9	99.9	99.9
Light bulb	96.7	79.2	93.1	95.0	94.5

TABLE IV
MAGNITUDE OF RANDOM NOISE FOR EACH HARMONIC

Harmonic	Input	Noise magnitude
Fundamental	1,2	0.3
3^{rd}	3,4	0.3
5^{th}	5,6	0.2
7^{th}	7,8	0.2
9^{th}	9,10	0.1
11^{th}	11,12	0.1
13^{th}	13,14	0.1
15^{th}	15,16	0.1

independent of each other, the current drawn by a combination of the devices should be equal to the sum of the current drawn by each. Based on this assumption, a new set of training data was created using the vector sums of the harmonics of individual devices to reduce the size of the training data set. The newly created training set was used for training the signature identification models while the original data set was used to test the SVM-based models as well as the RBF NN model. Because of the problems presented by the large number of local minima, the training and testing of the MLP-based models were repeated 100 times with different random initial weights. During this training, 66% of the original data set was used for validation stop (early stopping) to avoid overfitting. The remaining data were used for testing.

The results shown in Table III indicate that the developed models perform well with an average classification accuracy of about 85%. The drop in accuracy is greatly compensated by the ability of these models to perform classifications with information from only individual devices. This is a great step toward nonintrusive monitoring.

C. Training on Noisy Data Set

In the last stage of the experiments, noise at the magnitudes specified in Table IV was added to the original data set to test the ability of the developed classifiers on noisy data. The magnitudes were based on the amplitude of the current harmonics of individual devices. After adding the noise, the data set was split into training and testing sets with a 2:1 ratio. The random noise added was varied from 0.1 to 1.5 times the specified magnitude. For each step, training and testing were repeated 100 times with different random initial weights.

The results for the MLP-based model are shown in Fig. 6. Although the average accuracy slightly decreases with an increase

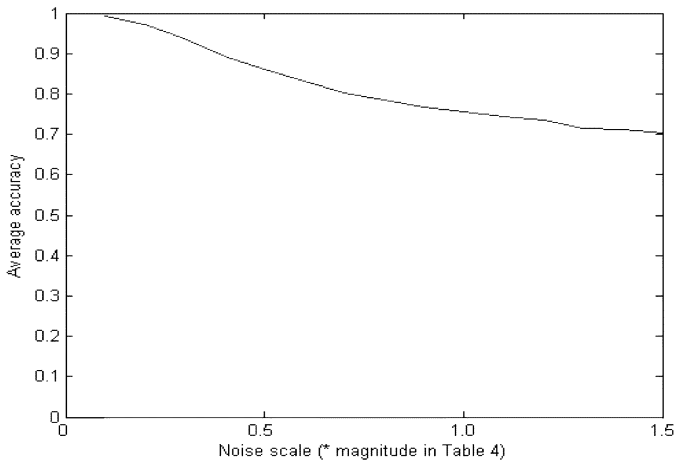

Fig. 6. Effect of random noise on classification accuracy.

TABLE V
CLASSIFICATION ACCURACY IN THE PRESENCE OF RANDOM NOISE

Device	Accuracy (%)				
	MLP	RBF	SVM		
			Linear	Polynomial	RBF
Monitor	88.3	71.8	89.0	89.0	88.3
CPU	71.2	63.8	71.4	71.4	71.4
Fluo. lamp	84.2	58.1	84.7	84.8	84.8
TV	68.0	52.7	64.7	64.7	65.0
Charger	66.8	53.1	66.1	66.5	66.1
Fan	59.5	50.3	61.6	62.0	61.5
Fridge	89.0	67.6	88.6	89.0	88.8
Light bulb	78.6	54.9	78.8	78.8	78.6

in the noise magnitude, it is noted that even at 1.5 times the magnitude, the average accuracy is above 70%.

Table V compares the classification accuracy of various models in the presence of noise. The results show that the models are capable of filtering noise that may be caused by unknown or faulty devices. It is noted that the performance of RBF-based models was not as good at that of the other classifiers.

Although the classification performance of MLP and SVM-based models was comparable, the MLP model had significantly lower computational resource requirements and was therefore used in further experiments. The RBF NN and SVM are limited by the size of the training set that can be used, while avoiding significant QP problems.

D. Experimental Setup With Ten Devices

In order to test the generalization capability of the MLP-based model classifier on other combinations of devices, two additional experiments with ten devices were set up. Due to the large number of possible combinations, only harmonic signatures of individual devices were measured. Using the mean values, the harmonic signatures for the combinations of devices were mathematically created. Random noise was added to simulate the fluctuations expected in the experimental measurements, and the resulting data set was used in the training set.

The first setup (set A) was tested by the experimental measurement of random combinations of the devices. The second setup (set B) was tested using mathematical combinations with

TABLE VI
CLASSIFICATION ACCURACY ON TEN-DEVICES SET A

No	Device	Accuracy (%)
1	Monitor	98.1
2	CPU	81.0
3	Fluorescent lamp	100
4	Television	71.4
5	Soldering iron	85.7
6	Fridge	100
7	Fan	75.2
8	Battery charger	70.5
9	Light bulb	90.5
10	Power drill	83.8

TABLE VII
CLASSIFICATION ACCURACY ON TEN-DEVICES SET B

No	Device	Accuracy (%)
1	PC CPU	99.5
2	PC Monitor	99.5
3	PC CPU (shutdown)	98.8
4	DC Power supply (0.1A)	83.5
5	DC Power supply (0.5A)	76.5
6	DC Power supply (0.25A)	73.0
7	DC Power supply (0.4A)	72.6
8	Notebook computer	99.3
9	Mobile phone charger	77.2
10	Fluorescent lamp	80.5

TABLE VIII
CLASSIFICATION ACCURACY ON THREE-PHASE DEVICES

No	Device	Accuracy (%)
1	Motor #1	87.5
2	Motor #2	99.9
3	Motor #2 with capacitors	97.7
4	Inverter #1	99.6
5	Inverter #2 (low frequency)	99.6
6	Inverter #2 (high frequency)	99.6
7	Fluorescent lamp without capacitor	65.1
8	Fluorescent lamp with capacitors	69.1

random noise. The training and testing were done on the MLP NN with a 16-20-10 configuration. Tables VI and VII show the test results of the first and second setup, respectively. The results are comparable to that of the eight-device setup.

E. Three-Phase Devices

Further experiments were conducted to test the applicability of the proposed harmonics signature identification approach to three-phase devices. Three-phase devices generally have more distinct signatures because of the additional information available from the other two phases.

The current harmonics of eight three-phase devices were measured using the Dranetz 8000-2 energy analyzer. With three phases and eight harmonics from each phase, there were a total of 48 inputs (real and imaginary) for each phase.

The training and testing sets containing combinations of devices were created mathematically in a manner similar to the ten-device setup explained above. Random noises of the magnitudes shown in Table IV were added to the harmonics of each phase to simulate random fluctuations and inaccurate representations of the current harmonics of various combinations of devices. An MLP NN with a 48-20-8 configuration was used to perform the classification. Table VIII presents test results. It is observed that the proposed classifiers correctly identify the devices from their harmonics signatures. The results are better than those of the eight-device single-phase tests due to the additional information present in the case of three-phase devices.

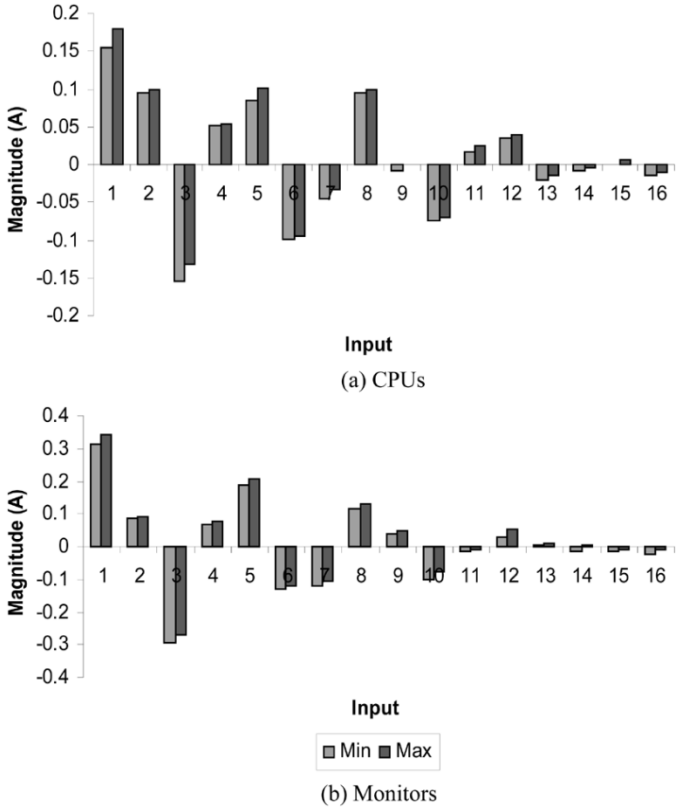

Fig. 7. Signature difference between devices of the same model. (a) CPUs. (b) Monitors.

F. Multiple Devices of the Same Model

In order to study the possibility of generalizing to devices of the same model and make, the harmonic signatures of multiples of the same device were compared.

Fig. 7 shows the difference between the harmonic signatures of four computer CPUs and four computer monitors of the same model. The figure indicates that the variations are smaller than the random noise magnitude in Table IV and are therefore within the generalization ability of the NN models. The models can potentially be used to identify multiple devices of the same model using the harmonics signature from only one of the devices. Consequently, it will not be likely for the model to be capable of distinguishing devices of the same model as distinct devices.

On the other hand, it should be noted that devices of the same nature or function, but different model or make (such as motor #1 and motor #2 in the three-phase devices set), are correctly identified because their harmonics signatures are usually significantly different.

VII. CONCLUSION

This paper has presented a novel approach to the identification of the devices present in an electrical installation based on the measurement of current at the incoming supply point. This new approach performs a black-box analysis to determine what

devices are possibly present—just by taking measurements from the electrical wiring that leads to the black box.

Several NN-based models were developed and tested for signature identification of electrical devices based on the current harmonics, even under noisy conditions. The results indicate that all models gave excellent classification performance and correctly identified the devices present in the experimental setup, establishing the applicability of the proposed approach.

Future research will include extending the scope to incorporate the various operational modes of each device and operation under different voltage sources. Research will also focus on the automatic detection of new devices, marking new regions of correspondence in the feature space, by setting thresholds to signify the presence of unknown devices.

REFERENCES

[1] J. Arrillaga, *Power System Harmonic Analysis*. New York: Wiley, 1997.

[2] W. Mack Grady and S. Santoso, "Understanding power system harmonics," *IEEE Power Eng. Rev.*, pp. 8–11, 2001.

[3] C. W. Smith Jr, "Power systems and harmonic factors," *IEEE Potentials Mag.*, vol. 20, no. 5, pp. 10–12, Dec. 2001/Jan. 2002.

[4] W. Tan and V. I. John, "Nonlinear fluorescent systems: their impact on power quality," in *Proc. Can. Conf.*, Sep. 25–28, 1994, pp. 144–147.

[5] M.-C. T. Nguyen and W. J. Lee, "An approach to enhance the harmonic sources identification process," in *Proc. IEEE Industrial Commercial Power Systems Technical Conf.*, 2000, pp. 127–132.

[6] G. T. Heydt, "Identification of harmonic sources by a state estimation technique," *IEEE Trans. Power Del.*, vol. 4, no. 1, pp. 569–576, Jan. 1989.

[7] Z. P. Du, J. Arrillaga, N. R. Watson, and S. Chen, "Identification of harmonic sources of power systems using state estimation," *Proc. Inst. Elect. Eng., Gen., Transm. Distrib.*, vol. 146, pp. 7–12, 1999.

[8] H. Ma and A. A. Girgis, "Identification and tracking of harmonic sources in a power system using a Kalman filter," *IEEE Trans. Power Del.*, vol. 11, no. 3, pp. 1659–1665, Jul. 1996.

[9] F. Sultanem, "Using appliance signatures for monitoring residential loads at meter panel level," *IEEE Trans. Power Del.*, vol. 6, no. 4, pp. 1380–1385, Oct. 1991.

[10] G. W. Hart, "Nonintrusive appliance load monitoring," *Proc. IEEE*, vol. 80, no. 12, pp. 1870–1891, Dec. 1992.

[11] C. Laughman, K. Lee, R. Cox, S. Shaw, S. Leeb, L. Norford, and P. Armstrong, "Power signature analysis," *IEEE Power Energy Mag.*, vol. 1, no. 2, pp. 56–63, Mar./Apr. 2003.

[12] S. Haykins, *Neural Networks—A Comprehensive Foundation*, NJ: Pearson Education, 1999.

[13] R. K. Hartana and G. G. Richards, "Constrained neural network-based identification of harmonic sources," *IEEE Trans. Ind. Appl.*, vol. 29, no. 1, Pt. 1, pp. 202–208, Jan./Feb. 1993.

[14] J. V. Wijayakulasooriya, G. A. Putrus, and P. D. Minns, "Electric power quality disturbance classification using self-adapting artificial neural networks," *Proc. Inst. Elect. Eng., Gen. Transm. Distrib.*, vol. 149, pp. 98–101, 2002.

[15] M. Rukonuzzaman and M. Nakaoka, "Magnitude and phase determination of harmonic currents by adaptive learning back-propagation neural network," in *Proc. IEEE Int. Conf. Power Electronics Drive Systems*, 1999, pp. 1168–1171.

[16] P. K. Dash, D. P. Swain, B. R. Mishra, and S. Rahman, "Power quality assessment using an adaptive neural network," in *Proc. Int. Conf. Power Electronics, Drives Energy Systems Industrial Growth*, vol. 2, 1996, pp. 770–775.

[17] S. Santoso, E. J. Powers, W. M. Grady, and A. C. Parsons, "Power quality disturbance waveform recognition using wavelet-based neural classifier—Part 1: Theoretical foundation," *IEEE Trans. Power Del.*, vol. 15, no. 1, pp. 222–228, Jan. 2000.

[18] L. S. Moulin, A. P. A. da Silva, M. A. El-Sharkawi, and R. J. Marks, "Support vector and multilayer preceptron neural networks applied to power systems transient stability analysis with input dimensionality reduction," in *Proc. Power Engineering Soc. Summer Meeting*, vol. 3, 2002, pp. 1308–1313.

[19] S. Poyhonen, M. Negrea, A. Arkkio, H. Hyotyniemi, and H. Koivo, "Fault diagnostics of an electrical machine with multiple support vector classifiers," in *Proc. IEEE Int. Symp. Intelligent Control*, 2002, pp. 373–378.

D. Srinivasan (M'89–SM'02) received the Ph.D. degree in engineering from the National University of Singapore (NUS).

Currently, she is an Associate Professor with the Department of Electrical and Computer Engineering, NUS. She was a Postdoctoral Researcher with the University of California at Berkeley from 1994 to 1995. Her research interest is in the application of soft computing techniques to engineering optimization and control problems.

W. S. Ng received the B.Eng. (Hons.) and M.Eng. degrees in electrical engineering from the National University of Singapore in 2002 and 2004, respectively.

Currently, he is a Lecturer in the Republic Polytechnic, Singapore.

A. C. Liew (M'72–SM'85) received the B.E. (Hons.) and Ph.D. degrees from the University of Queensland, Queensland, Australia, in 1969 and 1972, respectively.

Currently, he is a Professor in the Department of Electrical and Computer Engineering and Director of International Relations, National University of Singapore. From 1972 to 1979, he was with the Electrical Engineering Department, University of Malaya, Malaysia. His main interests are lighting and lightning protection, power quality, and power systems engineering.